Journal of Electrical and Computer Engineering Innovations
(JECEI)
Journal homepage: http://www.jecei.sru.ac.ir

Research paper

A Novel Analytical Approach for Time-response shaping of the PI controller in Field Oriented Control of the Permanent Magnet Synchronous Motors

H. Salimi, A. Zakipour*, M. Asadi
Department of Electrical Engineering, Arak University of Technology (AUT), Arak, Iran.

Article Info

Article History:
Received 23 December 2021
Reviewed 17 January 2022
Revised 11 April 2022
Accepted 11 April 2022

Keywords:
Permanent Magnet Synchronous Motor (PMSM)
Filed Oriented Control (FOC)
Controller tunning
Dynamic responses
Newton-Raphson numerical method

*Corresponding Author's Email Address: zakipour@arakut.ac.ir

Abstract

Background and Objectives: Permanent magnet synchronous motors (PMSM) have received much attention due to their high torque as well as low noise values. However, several PI blocks are needed for field, torque, and speed control of the PMSM which complicates controller design in the vector control approach. To cope with these issues, a novel analytical approach for time-response shaping of the Pi controller in the filed oriented control (FOC) of the PMSM is presented in this manuscript. In the proposed method, it is possible to design the controlling loops based on the pre-defined dynamic responses of the motor speed and currents in dq axis. It should be noted that as decoupled model of the motor is employed in the controller development, a closed loop system has a linear model and hence, designed PI controllers are able to stabilize the PMSM in a wide range of operation.
Methods: To design the controllers and choose PI gains, characteristic of the closed loop response is formulated analytically. According to pre-defined dynamic responses of the motor speed and currents in dq-axis e.g., desired maximum overshoot and rise-time values, gains of the controllers are calculated analytically. As extracted equation set of the controller tuning includes a nonlinear term, the Newton-Raphson numerical approach is employed for calculation of the nonlinear equation set. In addition, designed system is evaluated under different tests, such as step changes of the references. Finally, it should be noted that as the decoupled models are employed for the PMSM system, hence exact closed loop behavior of the closed loop system can be expressed via a linear model. As a result, stability of the proposed approach can be guaranteed in the whole operational range of the system.
Results: Controlling loops of the closed loop system are designed for speed control of the PMSM. To evaluate accuracy and effectiveness of the controllers, it has been simulated using MATLAB/Simulink software. Moreover, the TMS320F28335 digital signal processor (DSP) from Texas Instruments is used for experimental investigation of the controllers.
Conclusion: Considering the simulation and practical results, it is shown that the proposed analytical approach is able to select the controlling gains with negligible error. It has shown that the proposed approach for rise time and overshoot calculations has at most 0.01% for step response of the motor speed at 500 rpm.

Introduction

In recent years, permanent magnet synchronous motors (PMSM) have been used in a wide range of applications such as robotics, electric vehicles, aerospace, and

medical equipment [1] due to higher torque and lower noise, weight, and power loss compared to the induction motors with identical power rating [2].

Two main control approaches for closed loop control of the PMSM have been proposed in the literature. First method is called scalar control and basically it can be implemented by keeping the voltage to frequency ratio constant (V/f=constant).

In [3], this technique is employed in the PMSM. Even though the implementing of the scalar controller is straightforward in this condition, however its main drawbacks are complexity of the simultaneous control of speed and torque, as well as dynamic response control. For these reasons, scalar control is not a preferred choice in most of the applications.

The second approach for closed loop control of the electrical motors is vector control. Basically, two general techniques on vector control of the PMSM are reported: direct torque control (DTC) and field-oriented control (FOC).

Application of the DTC method on PMSM has been reported in [4], [5]. Main advantages of the DTC are simplicity of the implementation and acceptable dynamic response of the motor torque. On the other hand, its main drawbacks are variable switching frequency and high torque ripple which restricts widespread application of the mentioned approach [6]-[8].

On the other hand, FOC is widely used in industrial applications for closed loop control of the DC to AC inverters. In this method, AC machine can be assumed as a separately excited DC machine [9]. In other word, torque and speed of the electrical motor can be controlled separately if FOC approach is employed. Main advantages of the FOC method such as possibility of torque control at low speeds, and fast dynamic response of the speed loop make it more attractive for closed loop control of the AC motors in the industrial applications [10].

The FOC control system is implemented based on the separation of motor model in dq-axes. Actually, if the mentioned separation be possible in a closed loop system, a variety of controllers can be employed for speed/torque control of an electrical motor. For example, in [11], [12] the sliding mode controller is used according to FOC scheme.

Although the mentioned controllers can overcome the parameter's uncertainty challenges, however in [11], [12] chattering phenomena is seen in the controllers output signal which deteriorates advantages of the sliding mode technique.

In addition, in practical applications, the controller requires a high-speed processor and monitoring circuits which can considerably increase implementation costs of the practical system. In [13], [14], model reference adaptive control system has been developed for closed loop vector control the PMSM. The controller's parameters are optimally adjusted by using the PMSM model on different operational points. Moreover, implementation of the adaptive controller is a time consuming and complicated task.

In [15], [16] hysteresis current controller is used for FOC of the electrical motor. In ideal conditions, this controller has a zero steady-state error, however its main drawback is variable switching of the converter which complicates practical implementation of the hysteresis approach. In [17]-[19], model predictive controller is used for closed-loop control of the PMSM. Using this controller and by selecting an appropriate cost function, various goals can be achieved such as optimal system dynamics, switching frequency adjustment, etc., however, requirement of an accurate system model, uncertainty in model parameters, and time-consuming online calculation limit widespread application of the mentioned approach.

On the other hand, application of the linear PI controllers in the FOC structure has been increased particularly in industry applications [20]-[22]. Simplicity of the implementation has increased widespread application of the linear controllers. Actually, if a linear controller be tuned properly, it can stabilize the closed loop system and reject disturbances satisfactorily in an operating point.

In the FOC structure, three controllers are needed; two controllers are employed in the inner loop for dq currents adjustment, and the third controller in the outer loop generates the reference current of the inner loops.

To implement the FOC approach more efficiently by using the PI controllers, the proportional and integral coefficients must be selected properly for both inner and outer loops. One of the popular methods for selection of the control gains in closed-loop control of the PMSM is offline application of the innovative algorithms e.g. genetic [23], [24], PSO [25]-[27], and fuzzy logic [28]-[30]. Despite advantages of the mentioned training algorithms, large volume of real data is needed in training phase of the mentioned techniques. In addition, they may stick on the local optimum points and in other word, there is no guarantee that the mentioned search algorithms generate the globally optimum point and the best answer. In [31], [32] adaptive PI has been used for online calculation of the controller's coefficients. This method can be useful for systems in a wide range of operation. As mentioned, adaptive approaches are not an ideal choice for motor drive due to practical implementation issues as time-consuming on-line calculations are needed.

Regarding the PI controller tunning, various performance measures such as steady-state error, integral of absolute error, integral of square error, integral of time square error, and integral of time absolute error is defined [22], [33], [34]. Actually, the controller is designed so that to minimize one/some of the mentioned measures.

In this condition, if different controllers are employed for selection of the PI gains, it is possible to compare them in terms of the performance measure values. Hence, a superior approach will result in the minimum index regarding response rise time, settling time, and maximum overshoot.

However, in this manuscript, it should be noted that minimization of the mentioned indexes isn't employed for controller tuning.

Actually, a novel approach for time-response shaping of the closed loop system is developed in FOC of the PMSM. Regarding the pre-defined values of the overshoot and rise-time in the step response of the closed loop system, the PI gains are selected according to the numerical analysis of plant exact model. Clearly, if different values are selected as a design input (overshoot and rise-time) in the proposed method of this manuscript, different PI gains which demonstrate different performance indexes will be obtained.

In the meantime, to ensure the overall functionality of the controller, the design inputs (rise time and overshoot of the response) should be selected properly. For example, in this manuscript, desired overshoot and rise time of the speed controller are selected as 10% and 150ms and PI controller gains are calculated based on these values. Regarding the controller stability analysis which is added to the revised paper (please referrer the question 5), it is shown that the employed PI controller is stable despite large changes of the model parameters and uncertainties.

Briefly, this manuscript focuses on the time-response shaping and selection of the PI gains in FOC structure of the PMSM.

Gain selection algorithm is based on stability and robustness of the speed control loop. Due to application of the PI controller, elimination of the steady-state error and removal of the parameter's uncertainty issues, as well as input disturbance rejection will also be possible in the designed controllers.

Briefly, structure of the manuscript is as follows: In section II model of the PMSM is reviewed.

The PI controllers are designed for the inner and outer loops. Then selection of the controlling gains is explained in the third section.

Considering the XML-SE09MEKE PMSM, the performance of the proposed analytical approach for controller tuning is evaluated using a case study example in the next section. Finally, simulation and practical responses of the PMSM in different scenarios is evaluated in section V and conclusions are given in section VI.

Decoupled Model of the PMSM in FOC Approach

The mathematical model of PMSM in the *dq0* reference frame is expressed by the following differential equations, where the iron saturation, magnetic flux leakage, eddy current as well as hysteresis losses are assumed to be negligible [35]:

$$\frac{di_d(t)}{dt} = \frac{1}{L_d}\Big(v_d(t) - R_s i_d(t) + \omega_e(t) L_q i_q(t)\Big) \tag{1}$$

$$\frac{di_q(t)}{dt} = \frac{1}{L_q}\big(v_q(t) - R_s i_q(t) + \omega_e(t) L_d i_d(t) - \omega_e(t)\psi_r\big) \tag{2}$$

$$\frac{d\omega_e(t)}{dt} = \frac{P}{J_m}(T_e - \frac{B_v}{P}\omega_e(t) - T_L) \tag{3}$$

$$T_e = \frac{3}{2} P \psi_r i_q \tag{4}$$

where ω_e is the electrical speed of the motor, which depends on the rotor speed based on $\omega_e = P\omega_r$ and the parameter P refers number of motor poles pairs. Moreover, v_d and v_q represent the stator voltage and i_d and i_q are the motor current in the *dq* frame. It should be mentioned that T_L and T_e are the load and electromagnetic torques. Also, the parameters of the PMSM model include *dq*-axis inductances (L_d, L_q), field flux (ψ_r), stator resistance (R_s), motor inertia (J_m), and viscous coefficient (B_v).

Fig. 1(a) shows PMSM closed-loop speed control block diagram in which the PI blocks are responsible for control of the *dq*-axis currents in the inner loops and the speed controller of the outer loop. According to (1) and (2), it is seen that there is a nonlinear coherence between model state-variables on the *dq*-axis.

In other word, all the variables are dependent to each other and as a result, controlling loops cannot be employed directly which complicates closed loop system design.

To overcome this problem, it is well-known that the decoupling variables can be introduced as follows:

$$\frac{1}{L_d}\hat{v}_d = \frac{1}{L_d}\left(v_d + \omega_e L_q i_q\right) \tag{5}$$

$$\frac{1}{L_q}\hat{v}_q = \frac{1}{L_q}(v_q - \omega_e L_d i_d - \omega_e \psi_r) \tag{6}$$

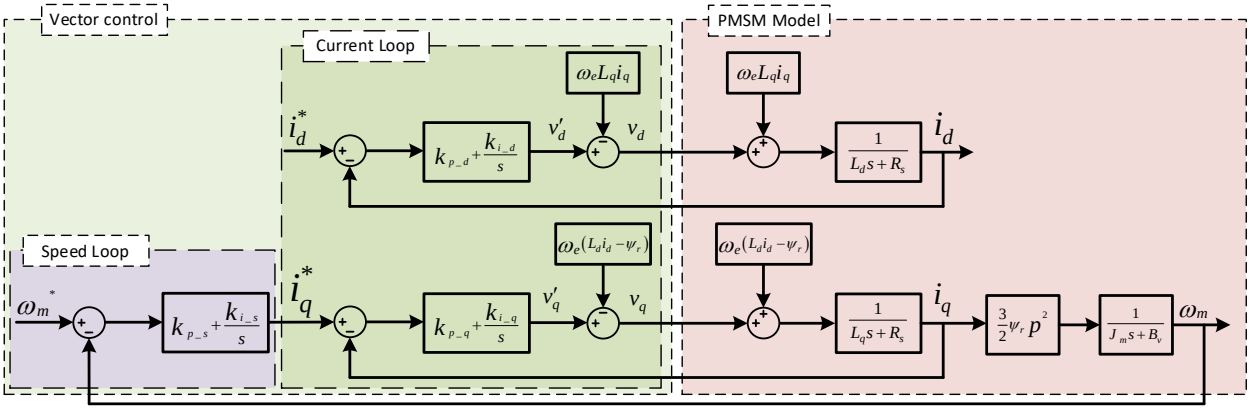

(a) Conventional current control

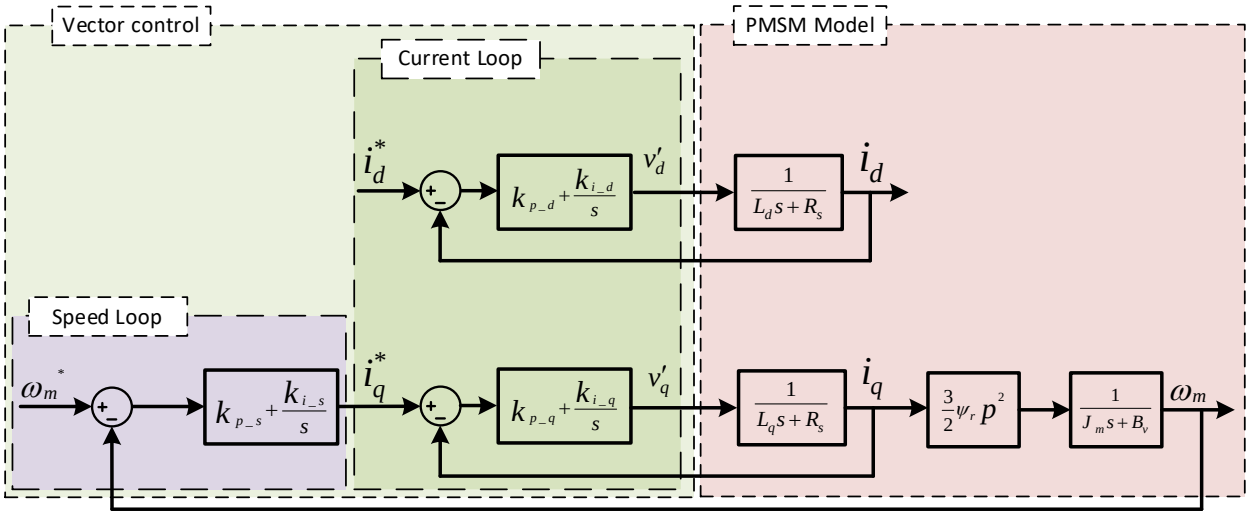

(b) Simplified decoupled FOC controller

Fig. 1: Closed-loop control of the speed controller in PMSM.

By replacing (5) and (6) in (1) and (2), the electrical equations of the motor can be rewritten as:

$$\frac{di_d}{dt} = -\frac{R_s}{L_d} i_d + \frac{1}{L_d}\hat{v}_d \tag{7}$$

$$\frac{di_q}{dt} = -\frac{R_s}{L_q} i_q + \frac{1}{L_q}\hat{v}_q \tag{8}$$

According to Fig. 1(b) and based on (7) and (8), two separate feedback control loops should be designed by adjustment of the $\hat{v}_d$ and $\hat{v}_q$ to achieve control target.

Analytical Approach for Controller's Tunning

Main objective of this manuscript is selection of the PI gains in FOC of the PMSM.

To address this issue, closed loop controller is implemented through different blocks e.g., inner and outer loops which is analyzed below.

A. Current Loop Design

To design the inner loops for *dq*-axes, considering proportional and integral gains as k_{p_d}, k_{i_d} and k_{p_q}, k_{i_q}, the PI controller of the *dq*-axis current can be written as:

$$\begin{aligned} v_d(t) = {} & k_{p\_d}\big(i_d{}^*(t) - i_d(t)\big) \\ & + k_{i\_d}\int_0^t \big(i_d{}^*(\tau) - i_d(\tau)\big)d\tau \\ & - \omega_e(t) L_q i_q(t) \end{aligned} \tag{9}$$

$$\begin{aligned} v_q(t) = {} & k_{p\_q}\left(i_q{}^*(t) - i_q(t)\right) \\ & + k_{i\_q}\int_0^t \left(i_q{}^*(\tau) - i_q(\tau)\right)d\tau \\ & + \omega_e(t) L_d i_d(t) - \omega_e(t)\psi_r \end{aligned} \tag{10}$$

By defining the virtual controller and according to Fig. 1(b) which shows simplified block diagram of the control

system, coupled mutual sentences of the model can be removed and hence, this technique facilitates controller design for PMSM. According to Fig. 1(b), to design the current PI controller, electrical term of the motor transfer functions in the frequency domain can be written as:

$$\frac{i_d(s)}{\hat{v}_d(s)} = \frac{\frac{1}{R_s}}{\frac{L_d}{R_s}s + 1} \tag{11}$$

$$\frac{i_q(s)}{\hat{v}_q(s)} = \frac{\frac{1}{R_s}}{\frac{L_q}{R_s}s + 1} \tag{12}$$

where $\hat{v}_d(s)$ and $\hat{v}_q(s)$ are auxiliary variables of the *dq*-axis voltages.

Considering the block diagram of the decoupled controller in Fig. 1(b), closed loop transfer function of the system can be calculated easily as:

$$G_{CL_C} = \frac{K_c(k_{i\_q} + k_{p\_q}s)}{\tau_C s^2 + (K_c k_{p\_q} + 1)s + K_c k_{i\_q}} \tag{13}$$

where $K_c = \frac{1}{R_s}$, $\tau_C = \frac{L_q}{R_s}$.

From (13), step response of close loop system in time domain is:

$$s_{CL\_C}(t) = \frac{(K_c k_{p\_q} - 1)\sinh(Wt)\, e^{(Yt)}}{2\tau_C W} - e^{(Yt)}\cosh(Wt) + 1 \tag{14}$$

where:

$$W = \frac{\sqrt{K_c^2 k_{p\_q}^2 + 2K_c k_{p\_q} - 4T_{sC} k_{i-_q} K_c + 1}}{2\tau_C} \tag{15}$$

$$Y = -\frac{(K_c k_{p\_q} + 1)}{2\tau_C} \tag{16}$$

According to (14), rise time can be calculated as:

$$t_{rise} = \frac{2\tau_C \log\left(-\frac{2\sqrt{(-K_c(k_{p\_q} - \tau_C k_{i\_q}))}}{H - K_c k_{p\_q} + 1}\right)}{H} \tag{17}$$

and

$$H = \sqrt{K_c^2 k_{p\_q}^2 + 2K_c k_{p\_q} - 4\tau_C k_{i-_q} K_c + 1} \tag{18}$$

It should be noted that the (14) expresses the step response of the closed loop system in time domain. According to time-derivative of the (14) and setting it into zero, time of the maximum point is obtained in (19).

This equation is calculated and simplified using the 'MATLAB symbolic analysis toolbox'. By replacing t_{MP} from (19) in (14), maximum value of the overshoot can be written as (20), where:

$$M = \sqrt{-\tau_C k_{i\_q}(k_{p\_q} - \tau_C k_{i\_q})} \tag{21}$$

$$N = k_{p\_q} - 2\tau_C k_{i-q} + K_c k_{p\_q}^2 - k_{p\_q} Q \tag{22}$$

$$Q = \sqrt{K_c^2 k_{p\_q}^2 + 2K_c k_{p\_q} - 4\tau_C K_c k_{i-q} + 1} \tag{23}$$

To calculate the controller coefficients, desired values of system rise time and maximum overshoot should be replaced in the (17) and (20).

As these equations are nonlinear, so it may be challenging task to introduce an analytical solution using the classical methods. On the other hand, numerical approaches e.g., the Newton-Raphson method can be employed to cope with the mentioned issues. The employed block diagram of the Newton-Raphson method is illustrated in Fig. 2.

According to Fig. 1(b), it is observed the current loop for *d*-axes is similar to *q*-axes. As a result, *d*-axes controller can be designed using the same equations if L_q is replaced with L_d.

$$t_{MP} = \tau_c * \log\left(-\frac{2 * \left(-k_{i\_q} * \tau_c * \left(k_{p\_q} - k_{i\_q} * \tau_c\right)\right)^{\frac{1}{2}}}{k_{p\_q} - 2 * k_{i\_q} * \tau_c + K_c * {k_{p\_q}}^2 - 2 * k_{p\_q} * \left(\frac{K_c^2 * {k_{p\_q}}^2}{4} + \frac{K_c * k_{p\_q}}{2} - k_{i\_q} * \tau_c * K_c + \left(\frac{K_c^2 * {k_{p\_q}}^2}{4} + \frac{K_c * k_{p\_q}}{2} - k_{i\_q} * \tau_c * K_c + \frac{1}{4}\right)^{\frac{1}{2}}\right)}\right) \tag{19}$$

$$MP = \frac{\frac{1}{2^{\frac{K_c k_{p-q}+1}{Q}}}\left(\tau_C k_{i-q} - k_{p-q} + 2^{\frac{K_c k_{p-q}+1}{Q}}\left(\frac{M}{N}\right)^{\frac{K_c k_{p-q}+1}{Q}} M\right)}{\left(\frac{M}{N}\right)^{\frac{K_c k_{p-q}+1}{Q}} M} - 1 \tag{20}$$

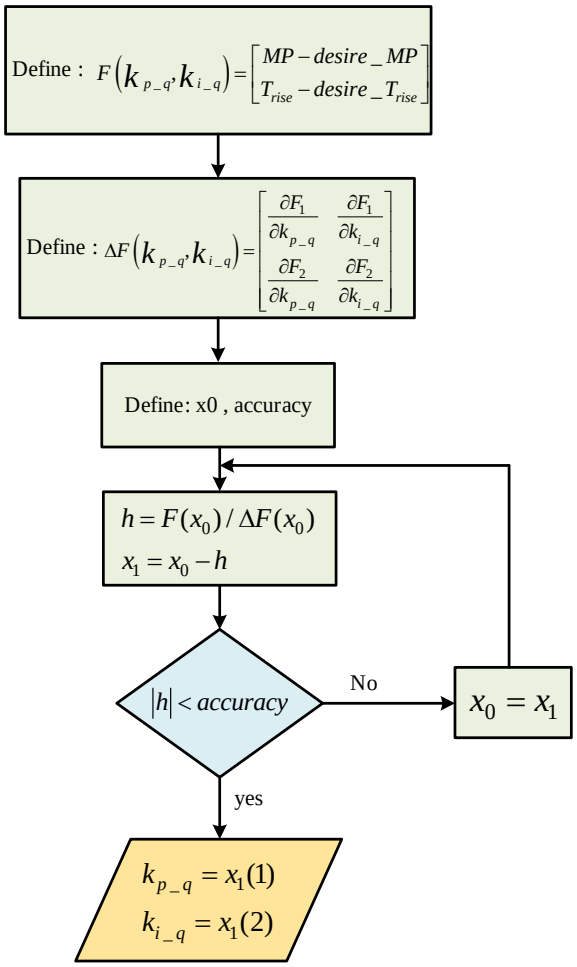

Fig. 2: Block diagram of the Newton-Raphson numerical method for calculation of the q-axes controlling gains.

B. Speed-Loop Design

Outer-loop of the introduced closed-loop system can be designed using the (3) and (4). These equations are used to describe mechanical behavior of the model as well as coherence between mechanical and electrical equations. By substituting (4) in (3), mechanical dynamic behavior of the PMSM can be described as:

$$\frac{d\omega_e(t)}{dt} = \frac{3}{2}\frac{P^2\psi_r}{J_m} i_q(t) + \frac{3}{2}\frac{P^2}{J_m}\left(L_d - L_q\right) i_d(t) i_q(t) - \frac{B_v}{J_m}\omega_e(t) - \frac{P}{J_m} T_L \quad (24)$$

The equation includes $\left(L_d - L_q\right)$ term. In non-salient pole PMSM, it is well known that $L_d = L_q$.

However, in salient motors where $L_d \neq L_q$, then $i_d(t)$ should be set to zero in the control system.

So, in both conditions, the second term of the equation $(\frac{3}{2}\frac{P^2}{J_m}\left(L_d - L_q\right) i_d(t) i_q(t))$ will be zero.

Also, $\frac{B_v}{J_m}\omega_e(t) - \frac{P}{J_m} T_L$ term in the (24) is directly related to the load torque on the motor shaft. This parameter can be considered as a disturbance during the controller operation.

Hence, if an integrator is employed in the outer speed controller, steady-state error can be eliminated. In this condition, (24) can be rewritten as in frequency domain:

$$\left(s + \frac{B_v}{J_m}\right)\omega_e(s) = \frac{P^2\psi_r}{J_m} i_q(s) \quad (25)$$

According to Fig. 1(b), by substituting (15) into (25), speed transfer function to the reference current signal of the *q*-axis can be written as:

$$\frac{\omega_e(s)}{i_q^*(s)} = \left(\frac{\frac{3}{2}\frac{P^2\psi_r}{J_m}}{s + \frac{B_v}{J_m}}\right) G_{CL\_C} \quad (26)$$

In (26), it is seen that $s = -\frac{B_v}{J_m}$ is related to mechanical behavior of the system and hence it can be assumed as a dominant pole of the closed loop system. So, for outer speed loop, closed loop transfer function of the system can be written as follow:

$$G_{CL_S} = \frac{K_M\left(k_{i\_s} + k_{p\_s} s\right)}{\tau_M s^2 + \left(K_M k_{p\_s} + 1\right)s + K_M k_{i\_s}} \quad (27)$$

where:

$$K_M = \frac{3}{2}\frac{P^2\psi_r}{J_m} \quad (28)$$

$$\tau_M = \frac{J_m}{B_v} \quad (29)$$

As transfer function of the current loop in (13) is similar to (27), hence, similar approach which is presented for numerical solution of the inner loop in Fig. 2, can be employed for outer speed controller design based on the desired rise time and maximum overshoot values.

Case Study for XML-SE09MEKE PMSM

In this section, developed approach is employed for XML-SE09MEKE PMSM from LS Electric Company. The performance of the proposed analytical approach for controller tuning is evaluated using a case study example.

The nominal parameters of the tested closed loop system including motor and inverter parameters are listed in Table 1.

*A. Case-1- Selection of the controller gains for a constant **MP** and several different t_r values in the inner current loop*

Assuming a fixed overshoot in the controller's response, step response and bode diagram of the closed loop system is shown in Fig. 3 for several rise time values. Obtained controller gain for each rise time value is listed in Table 2.

It is observed that the controller gain tuning algorithm has an acceptable error. Maximum value of the error in this test is less than 7.5%. Also, according to gain and phase margins of the inner-loop in Table 2 as well as in Fig. 3, it can be concluded that the control system is able to stabilize the closed-loop plant in the mentioned operating point.

Table 1: Inverter and XML-SE09MEKE PMSM parameters

Parameter	Symbol	**Unit**	Value
Rated Power	P_n	W	900
Rated Torque	T_{en}	N.m.	8.59
Rated Speed	w_n	RPM	1000
Voltage DC Link	Vdc	V	310
Pole pairs	P	-	4
Stator Resistance	R_s	Ω	1
Stator inductance	L_s	mH	7.5
Electrical Back EMF Constant	ψ_m	wb	0.3108
Rotor Inertia	J_m	$kg.m^2$	20.6e-4
viscous coefficient	B_v	$kg.m$^2 /s	0.0001
Maximum Current	I_{max}	A	5.2
Sampling Time	T_s	μs	25
Switching Frequency	f_{sw}	KHz	40
IGBT Driver	UCC2154a Texas Instrument		
IGBT	40N120FL2		

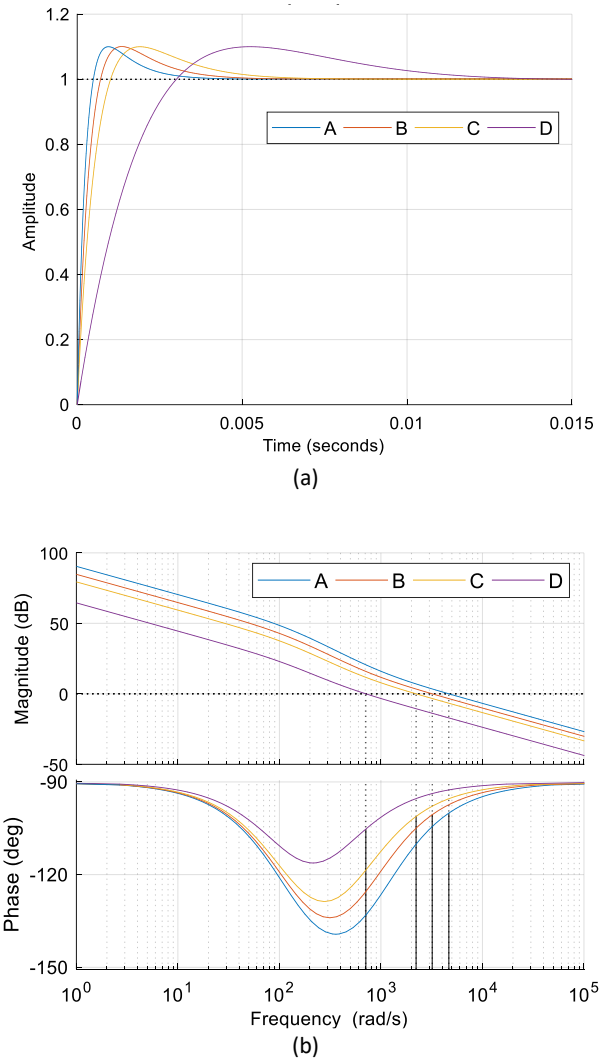

Fig. 3: Step response (a) and bode plot (b) of the inner loop for several different rise time values using a constant overshoot.

Table 2: Selected controller gains for several different rise time values and a constant overshoot

No.	MP (%)	Rise time (ms)*			Margins Value**		Current loop PI parameters	
		t_r^d	t_r^m	Err. (%)	GM (dB)	PM (deg)	k_{i_c}	k_{p_c}
A	10	0.5	0.48	4	Inf	79.91	33209	34.8
B	9.998	0.8	0.74	7.5	Inf	79.47	17287	23.4
C	10	1	0.95	5	Inf	78.83	9337	16.14
D	9.98	3	3.1	3.33	Inf	74.76	1682	4.88

*t_r^d:desired rise time t_r^m: measured rise time
** GM: Gain Margin PM: Phase Margin

B. *Case-2- Selection of the controller gains for a constant t_r and several different MP values in the inner current loop*

In accordance with the previous test in case-1, controller gains are tuned based on a constant rise-time value. Step response and bode diagram of the closed loop system in case-2 is shown in Fig. 4 for different MP values. Obtained controller gain for each condition is listed in Table 3. Maximum error value in this case is less than 0.2%.

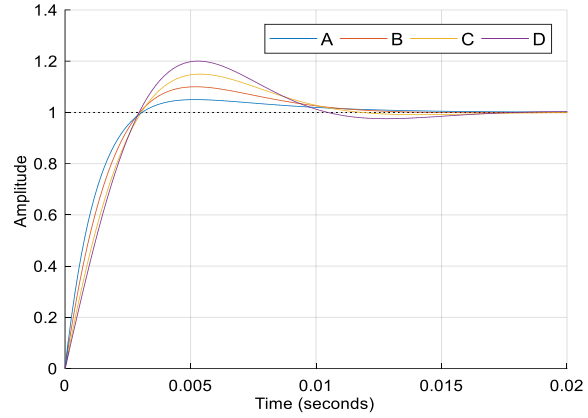

(a) Step response

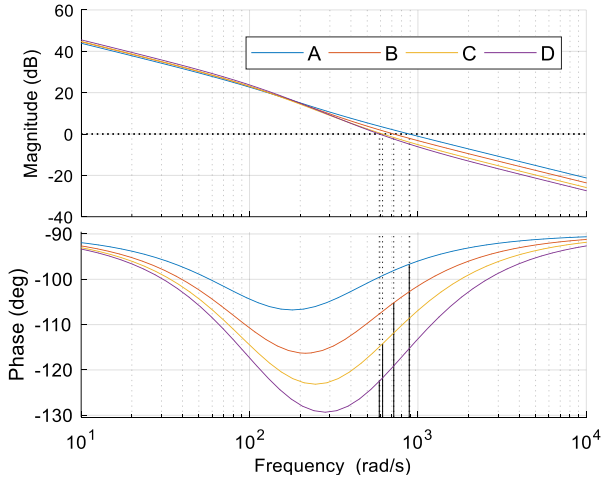

(b)Bode diagram

Fig. 4: Response of the inner-current loop in case-2.

Table 3: Selected controller gains in case-2

No.	t_r (ms)	overshoot (%)*		Margins Value**			Current loop PI parameters	
		MP^d	MP^m	Err. (%)	GM (dB)	PM (deg)	k_{i_c}	k_{p_c}
A	3.06	5	4.99	0.2	Inf	83.32	1569	6.53
B	2.98	10	9.99	0.1	Inf	74.82	1707	4.94
C	3.07	15	14.99	0.06	Inf	65.69	1733	3.81
D	2.95	20	19.99	0.05	Inf	57.55	1897	3.19

*MP^d:desired overshoot MP^m: measured overshoot
** GM: Gain Margin PM: Phase Margin

In order to study the outer speed loop, step response of the current loop for selected controller gains is shown in Fig. 5.

In this condition, desire values of maximum overshoot and rise time are selected equal to 10% and 3 milliseconds, respectively.

As a result, according to the proposed tuning algorithm, 9.99% overshoot and 2.9 milliseconds rise-time are achieved respectively.

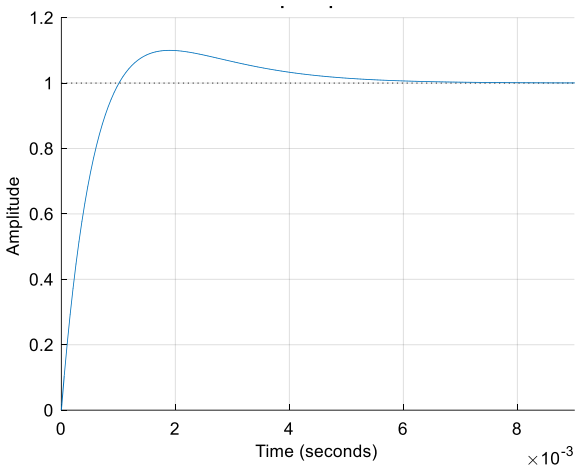

Fig.5: step response of the inner loop based on the selected controller gains

C. *Case-3- Selection of the controller gains for a constant MP and several different t_r values in the outer speed loop*

Fig. 6 shows step response and bode diagram of designed controller for a constant overshoot (10%) and variable rise time. Results of this test is shown in Table 4. According to the Table 4, the maximum value of the desired rise time is close to the real values. Maximum error in this test is less than 2.3%. Also, values of gain and phase margins in Table 4 and Fig. 6 illustrate stability of control system in these conditions.

Table 4: Controller parameters in case-3

No.	MP (%)	Rise time (ms)*		Margins Value**			Current loop PI parameters	
		t_r^d	t_r^m	Err. (%)	GM (dB)	PM (deg)	k_{i_s}	k_{p_s}
A	10.02	20	19.78	1.1	25	79.9	0.536	0.0286
B	10.01	80	79.81	0.2	37.4	80.5	0.034	0.0071
C	9.99	150	150.1	0.1	43	80.6	0.01	0.0038
D	10.5	250	255.8	2.3	47.9	80.5	0.003	0.0021

*t_r^d:desired rise time t_r^m: measured rise time
** GM: Gain Margin PM: Phase Margin

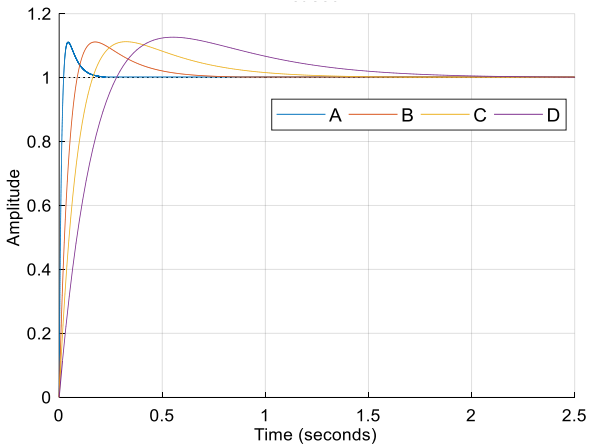

(a)

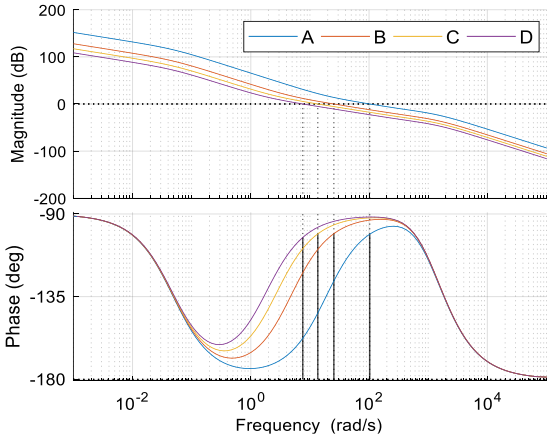

(b)

Fig. 6: Step response (a) and bode diagram (b) of the outer loop in case-3.

D. Case-4- Selection of the controller gains for a constant t_r and several different MP values in the outer speed loop

Similar to the previous test in case-3, controller gains are tuned based on a constant rise-time (50ms) value in case-4 and step response and bode diagram of the closed loop system are shown in Fig. 7 for different MP values. Obtained controller gain for each condition is listed in Table 5. Maximum error value in this case is less than 0.45%.

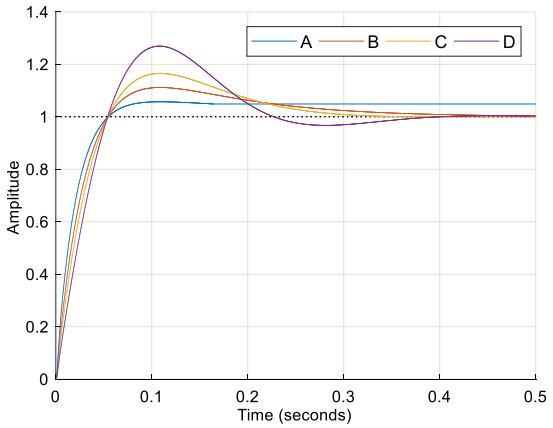

(a)

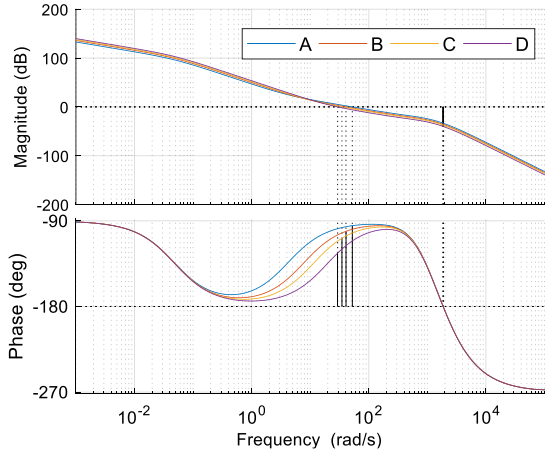

(b)

Fig. 7: step response (a) and bode diagram (b) of the outer loop in case 4.

Table 5: controller parameters in case-4

No.	t_r (ms)	overshoot (%)*			Margins Value**		Current loop PI parameters	
		MP^d	MP^m	Err. (%)	GM (dB)	PM (deg)	k_{i_s}	k_{p_s}
A	49.7	5	5	0	31	85.7	0.0609	0.0148
B	49.7	10	10.02	0.2	33.2	80.4	0.0869	0.0114
C	49.8	15	15.05	0.4	34.8	73.8	0.1061	0.0094
D	49.8	25	25.11	0.44	37.4	58.6	0.1352	0.0069

*MP^d:desired overshoot MP^m: measured overshoot
** GM: Gain Margin PM: Phase Margin

Results and Discussion

In this section, validation of the vector control approach is studied based on the selected controller gains under different scenarios. Experiments are conducted out using the XML-SE09MEKE three-phase PMSM from *LS Electric*.

A. Simulation Result

In this study, currents of the *dq*-axes, control signal and speed of the machine are shown in Fig. 8 based on simulation of the designed closed loop system in MATLAB/Simulink software.

Desired values of maximum overshoot and rise time are selected as 15% and 100ms respectively. From the simulation results in Fig. 8, it is seen that these variables are equal to 16% and 98ms which are properly compatible.

Furthermore, it is shown that the control signal ($\mathbf{U}_{\mathrm{abc}}$) is quite stable.

Also, currents of the *dq*-axes can follow their

reference values with an acceptable transient response and zero steady-state error.

Moreover, in the Fig. 8, the three-phase motor input voltages ($\mathbf{V}_{\mathrm{Line-abc}}$) which are supplied through the inverter is illustrated.

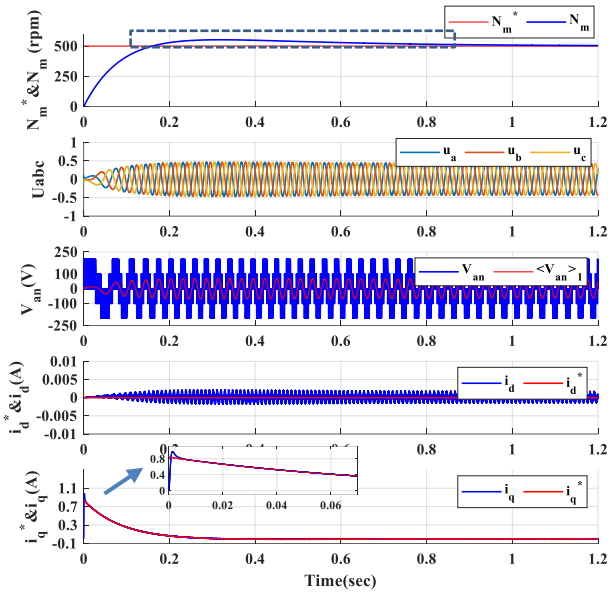

Fig. 8: Simulation of the designed closed loop system in MATLAB/Simulink.

In this paper, a proportional-integral linear controller is designed for FOC control of the PMSG.

It is well known that integral term can suppress the steady-state error of the closed loop control system despite uncertainty of the model parameters which has been demonstrated in the following simulation results. Also, regarding the robustness analysis, it can be considered as the stability of the closed-loop controller in case of uncertainties.

Actually, model of the plant, which is employed for controller design, may include some differences respect to the practical system due to inherent tolerance of the parameters, un-modelled dynamics, and nonlinearities. Hence, robustness analysis is a vital issue during the controller design.

Time-response of the designed controllers for step changes of the motor intertie, friction (viscous) coefficient, load torque, stator series resistance and inductance are shown in Fig. 9.

All the motor parameters are stepped up from the normal operating point to the two-times of nominal values.

Despite changes of the system operating point in a wide range, it can be concluded that the designed controller is stable and robust with respect to parameters changes.

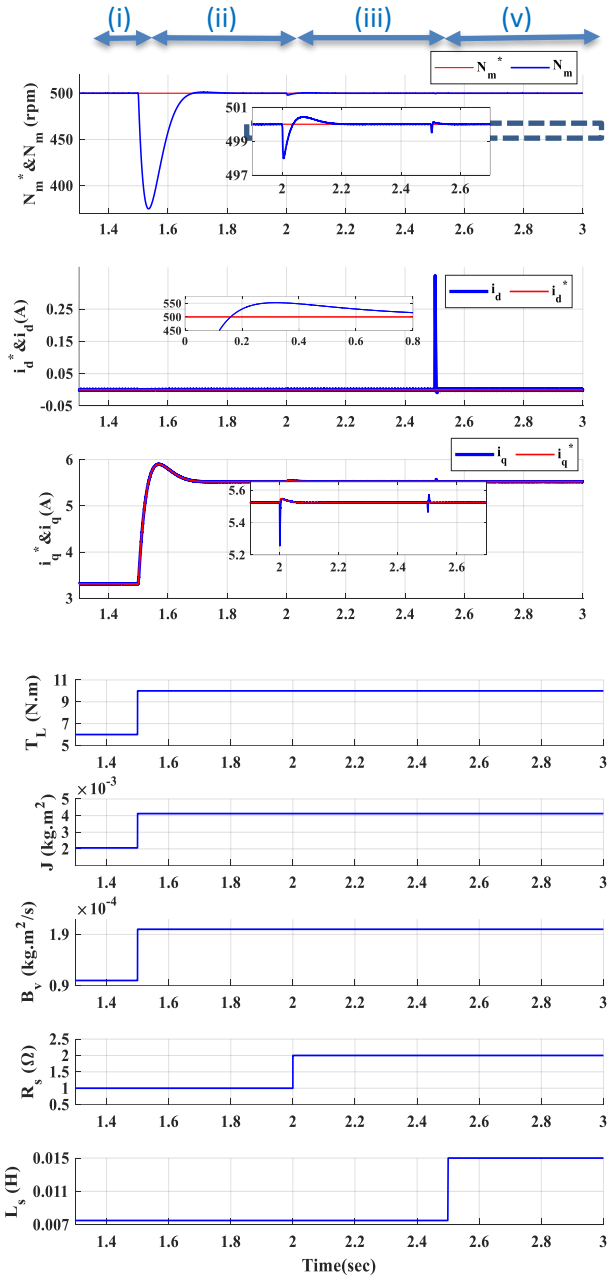

Fig. 9: Time response of the designed controllers for step changes of the motor intertie, load torque, stator series resistance and inductance.

B. *Experimental results*

The experimental test bench which is employed for evaluation of the designed controller based on Table 1, is shown in Fig. 10.

The proposed FOC algorithm is implemented using the TMS320F28335 DSP board from *Texas Instruments*. A 3000 pulse per round embedded encoder is adopted for measurement of the rotor position and speed feedback signals.

In order to plot the measured waveforms, a serial interface is employed for data transfer between DSP and computer.

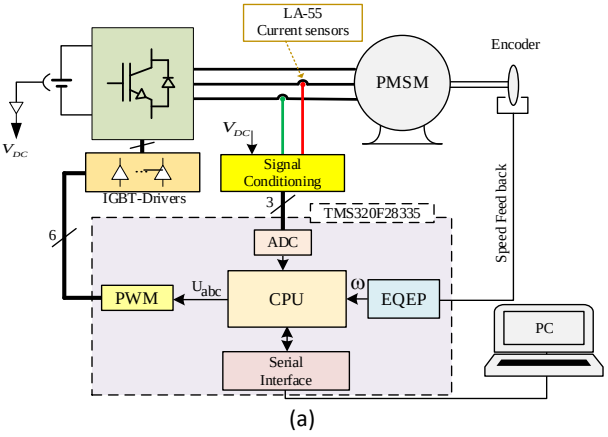

Fig. 10: Block diagram of the experimental setup (a) and photo of the test bench (b).

Test 1- Experimental response of the closed loop system for different gains

According to different design conditions in Table. 6, experimental step response of the developed closed loop system for outer speed loop is shown in Fig. 11. Accuracy of the developed algorithm is evaluated in three different cases (A, B and C).

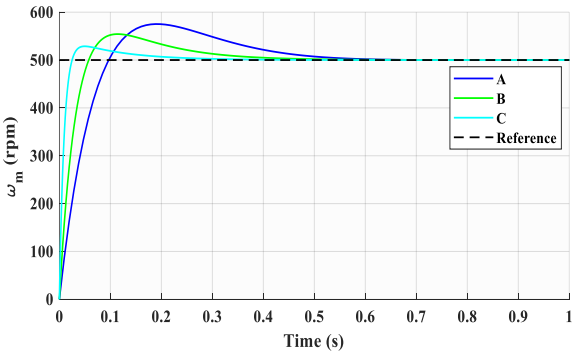

Fig. 11: Experimental response of the outer-control loop for different design conditions

Test 2- Experimental start-up response

In Fig. 12, experimental response of the designed closed loop system is illustrated during start-up and steady-state conditions. In this test, desired values of the maximum overshoot and rise time are assumed as 15% and 100ms respectively. So, as it is written in Table. 6, controller gains will be equal to $k_{p\_s} = 0.0346$ and $k_{i\_s} = 0.2163$ for the speed loop. According to the experimental response, it is seen that measured values for the mentioned parameters are 14% and 97ms, respectively which is compatible with design criteria. Also, controller has a negligible error during the steady-state condition.

Table 6: Summary of the experimental results in test-1

No.	overshoot (%)*			Rise time (ms)**			Current loop PI parameters	
	MP^d	MP^m	Err. (%)	t_r^d	t_r^m	Err. (%)	k_{i_s}	k_{p_s}
A	15	15.07	0.47	100	96	4	0.0346	0.2163
B	10	10.85	8.5	50	57	14	0.0687	0.5092
C	5	5.74	14.8	25	24.7	1.2	0.2048	1.9086

*MP^d:desired overshoot MP^m: measured overshoot
**t_r^d:desired rise time t_r^m: measured rise time

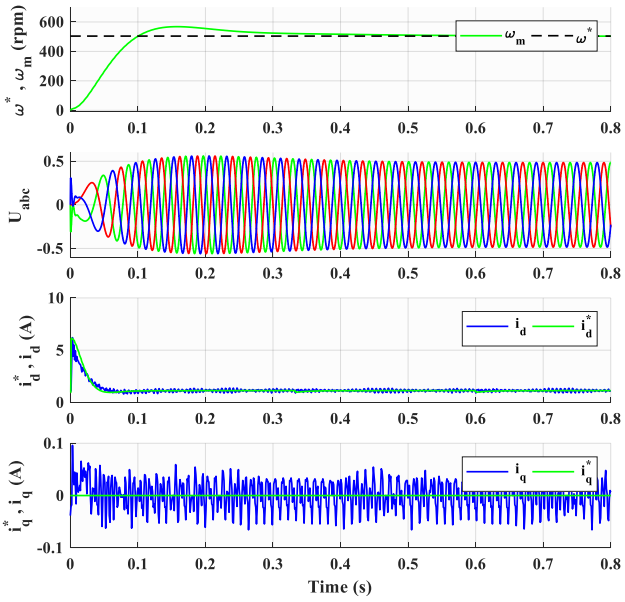

Fig. 12: Experimental response of the controller during start-up.

Test 3- Dynamic response of the controllers

To verify stability of the proposed system in different operating points, speed reference of the closed-loop control system is stepped between 350 and 500 rpm in test-3.

In spite of step changes of speed reference in a wide range in Fig. 13, it is seen that both inner and outer loops are stable during transients with zero steady-state error. In this test, similar gains are used for both inner and outer loops of the controller.

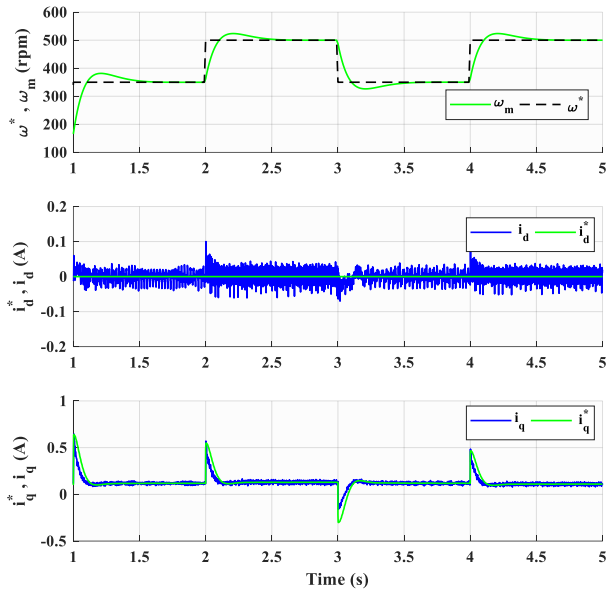

Fig. 13: Experimental dynamic response of the designed closed loop system.

Conclusion

In this manuscript, a novel method for tuning of the PI gains in FOC structure of the PMSM drivers is presented. The proposed method enjoys fast calculation time, so it can be employed in wide ranges of application *e.g*. CNC machine and electric vehicles.

In this method, the rise time and maximum overshoot values can be employed separately for tuning of the controller. Designed technique employs the Newton Raphson method to solve the nonlinear equations of the model.

The stability of the proposed method has also been evaluated by using the bode plot analysis. According to simulation and experimental results in different operational conditions, the proposed inner-current and outer-speed loops have stable and robust responses with zero steady-state error.

Author Contributions

This paper is the result of H. Salimi's M.Sc. thesis supervised by A. Zakipour and advised by A. Asadi. All of the authors have the same contribution in different parts of the manuscript including system modeling, controller design, simulation and experimental.

Acknowledgment

The author gratefully acknowledges the Power Quality Lab of Arak University of Technology.

Conflict of Interest

The author declares that there is no conflict of interests regarding the publication of this manuscript. In addition, the ethical issues, including plagiarism, informed consent, misconduct, data fabrication and/or falsification, double publication and/or submission, and redundancy have been completely observed by the authors.

Abbreviations

PMSM	Permanent Magnet Synchronous Motor
PWM	Pulse Width Modulation
PI	Proportional Integral
FOC	Field Oriented Control

References

[1] S. Khodakaramzadeh, M. Ayati, M. Haeri Yazdi, "Fault diagnosis of a permanent magnet synchronous generator wind turbine," J. Electr. Comput. Eng. Innovations, 9(2): 143-152, 2021.

[2] M.E. Gerlach, M. Zajonc, B. Ponick, "Mechanical stress and deformation in the rotors of a high-speed PMSM and IM," e & i Elektrotech. Informationstech., 138: 96-109, 2021.

[3] W.J. Kim, S.H. Kim, "MTPA operation scheme with current feedback in V/f control for PMSM drives," Journal Power Electron., 20: 524-537, 2020.

[4] H. Mesloub, R. Boumaaraf, M.T. Benchouia, A. Goléa, N. Goléa, K. Srairi, "Comparative study of conventional DTC and DTC_SVM based control of PMSM motor—Simulation and experimental results," Math. Comput. Simul., 167: 296-307, 2020.

[5] S.J. Kim, J. Park, D.H. Lee, "Zero voltage vector-based predictive direct torque control for PMSM," in Proc. 2019 IEEE Student Conference on Electric Machines and Systems (SCEMS 2019): 1-6, 2019.

[6] D. Ahmed, B. Mokhtar, B. Aek, "DTC hybrid control by different methods of observation with artificial intelligence for induction machine drives," Int. J. Power Syst., 10(4), 2019.

[7] S. Khateri-Abri, F.Y. Notash, S. Tohidi, "A reduced-switch 3-level vsi based direct torque control of PMSM," in Proc. 2019 27th Iranian Conference on Electrical Engineering (ICEE): 565-569, 2019.

[8] M. Alizadeh Pahlavani, H. Damroodi, "LPV Control for speed of permanent magnet synchronous motor (PMSM) with PWM Inverter," J. Electr. Comput. Eng. Innovations, 4: 185-193, 2016.

[9] A. Kushwaha, M. Gopal, "Reinforcement learning-based controller for field-oriented control of induction machine," Soft Computing for Problem Solving, ed: Springer, 737-749, 2019.

[10] R. Marouane, Z. Malika, "Particle swarm optimization for tuning PI controller in FOC chain of induction motors," in Proc. 2018 4th International Conference on Optimization and Applications (ICOA): 1-5, 2018.

[11] X. Wang, M. Reitz, E.E. Yaz, "Field oriented sliding mode control of surface-mounted permanent magnet AC motors: Theory and applications to electrified vehicles," IEEE Trans. Veh. Technol., 67: 10343-10356, 2018.

[12] A. Zakipour, N. Ghaffari, M. Salimi, "State space modeling and sliding mode current control of the grid connected multi-level flying capacitor inverters," J. Electr. Comput. Eng. Innovations, 9(2): 215-228, 2021.

[13] A.T. Nguyen, M.S. Rafaq, H.H. Choi, J.W. Jung, "A model reference adaptive control based speed controller for a surface-mounted permanent magnet synchronous motor drive," IEEE Trans. Ind. Electron., 65: 9399-9409, 2018.

[14] A. Chouya, M. Chenafa, A. Mansouri, "Adaptive field-oriented control with MRAC regulator for the permanent magnet synchronous motor," Int. J. Control Syst. Rob., 4: 52-57, 2019.

[15] J. Zhang, H. Yang, T. Wang, L. Li, D.G. Dorrell, D.D.C. Lu, "Field-oriented control based on hysteresis band current controller for a permanent magnet synchronous motor driven by a direct matrix converter," IET Power Electron., 11: 1277-1285, 2018.

[16] M. Sreejeth, M. Singh, "Performance analysis of PMSM drive using hysteresis current controller and PWM current controller," in Proc. 2018 IEEE International Students' Conference on Electrical, Electronics and Computer Science (SCEECS): 1-5, 2018.

[17] S. Wang, D.D. Xu, C. Li, "Dynamic control set-model predictive control for field-oriented control of VSI-PMSM," in Proc. 2018 IEEE Applied Power Electronics Conference and Exposition (APEC): 2630-2636, 2018.

[18] W. Zhang, W. Yang, W. Yan, D. Xu, "Improved finite control set model predictive control for permanent magnet synchronous motor drives," in Proc. 2019 Chinese Control Conference (CCC): 2977-2982, 2019.

[19] Y. Ahmed, A. Hoballah, E. Hendawi, S. Al Otaibi, S.K. Elsayed, N.I. Elkalashy, "Fractional order PID controller adaptation for PMSM drive using hybrid grey wolf optimization," Int. J. Power Electron. Drive Syst. (IJPEDS), 12: 745-756, 2021.

[20] H. Celik, T. Yigit, "Field-oriented control of the PMSM with 2-DOF PI controller tuned by using PSO," in Proc. 2018 International Conference on Artificial Intelligence and Data Processing (IDAP): 1-4, 2018.

[21] O. EROL, M. AKTAŞ, Y. ALTUN, "Obtaining of PI control parameters for vector controlled PMSM," in Proc. Int. Conf. Hydraul. Pneum. Tools, Seal. Elem. Fine Mech. Specif. Electron. Equip. Mechatronics, 2017.

[22] F. Jamshidi, M. Vaghefi, "WOA-based interval type II fuzzy fractional-order controller design for a two-link robot arm," J. Electr. Comput. Eng. Innovations, 7: 69-82, 2018.

[23] G. Demir, R.A. Vural, "Speed control method using genetic algorithm for permanent magnet synchronous motors," in Proc. 2018 6th International Conference on Control Engineering & Information Technology (CEIT): 1-6, 2018.

[24] H. Chaoui, M. Khayamy, O. Okoye, H. Gualous, "Simplified speed control of permanent magnet synchronous motors using genetic algorithms," IEEE Trans. Power Electron., 34: 3563-3574, 2018.

[25] A.A. Abd Samat, M. Zainal, L. Ismail, W.S. Saidon, A.I. Tajudin, "Current PI-gain determination for permanent magnet synchronous motor by using particle swarm optimization," Ind. J. Electric. Eng. Comput. Science, 6: 412-421, 2017.

[26] T. M. Reda, K.H. Youssef, I.F. Elarabawy, T.H. Abdelhamid, "Comparison between optimization of PI parameters for speed controller of PMSM by using particle swarm and cuttlefish optimization," in Proc. 2018 Twentieth International Middle East Power Systems Conference (MEPCON): 986-991, 2018.

[27] R. Pilla, T.S. Gorripotu, A.T. Azar, "Tuning of extended Kalman filter using grey wolf optimisation for speed control of permanent magnet synchronous motor drive," Int. J. Autom. Control, 15: 563-584, 2021.

[28] D. Gu, Y. Yao, D.M. Zhang, Y.B. Cui, F.Q. Zeng, "Matlab/simulink based modeling and simulation of fuzzy PI control for PMSM," Procedia Computer Science, 166: 195-199, 2020.

[29] S. Sakunthala, R. Kiranmayi, P.N. Mandadi, "Investigation of PI and fuzzy controllers for speed control of PMSM motor drive," in Proc. 2018 International Conference on Recent Trends in Electrical, Control and Communication (RTECC): 133-136, 2018.

[30] W.A.A. Salem, G. F. Osman, S.H. Arfa, "Adaptive neuro-fuzzy inference system based field oriented control of PMSM & speed estimation," in Proc. 2018 Twentieth International Middle East Power Systems Conference (MEPCON): 626-631, 2018.

[31] S.C. Chen, H.K. Hoai, "Studying an adaptive fuzzy PID controller for PMSM with FOC based on MATLAB embedded coder," in Proc. 2019 IEEE International Conference on Consumer Electronics-Taiwan (ICCE-TW): 1-2, 2019.

[32] P.Q. Khanh, H.P. H. Anh, C.V. Kien, "Advanced sensor-less control of IPMSM motor using adaptive neural FOC approach," Applied Mechanics and Materials: 149-157, 2019.

[33] B. Verma, P.K. Padhy, "Robust fine tuning of optimal PID controller with guaranteed robustness," IEEE Trans. Ind. Electron., 67: 4911-4920, 2019.

[34] Q. Xu, C. Zhang, L. Zhang, C. Wang, "Multiobjective optimization of PID controller of PMSM," J. Control Scie. Eng., 2014: 1-10, 2014.

[35] R. Krishnan, Permanent magnet synchronous and brushless DC motor drives: CRC press, 2017.

Biographies

Hesam Salimi was born in Iran, 1995. He received his B.S. and M.S. degrees in power Electrical Engineering from Arak University of Technology (ArakUT), Arak, Iran, in 2018 and 2021, respectively. His research interests include design and control of the DC/DC and DC/AC converter, switching power supplies and Electrical Machine drive.

- Email: h.salimi1995@gmail.com
- ORCID: 0000-0002-7937-9222
- Web of Science Researcher ID: NA
- Scopus Author ID: NA
- Homepage: NA

Adel Zakipour was born in Iran, in 1981. He received his Ph.D. degrees in Electrical Engineering from K.N.Toosi University of technology, Tehran, Iran, in 2017. Currently, he is an assistant professor in power electronics at department of electrical engineering, Arak university of technology. His research interests include design and control of the DC/DC and DC/AC converter, grid connected inverters and variable speed drive.

- Email: zakipour@arakut.ac.ir
- ORCID: 0000-0003-4900-5841
- Web of Science Researcher ID: 4236434
- Scopus Author ID: 55613351600
- Homepage: http://arakut.ac.ir/fa/zakipur.html

Mehdi Asadi was born in Iran, 1979. He received the B.Sc., M.Sc., and Ph.D. degrees in electrical engineering from Iran University of Science and Technology (IUST), Tehran, Iran, in 2002, 2004, and 2013, respectively. Since 2013, he has jointed to the Arak University of Technology, Arak, Iran. His research interests include high-power and high-frequency converters, electrical machines drives, power quality, battery chargers, and FACTS devices.

- Email: m.asadi@arakut.ac.ir
- ORCID: 0000-0001-7342-1584
- Web of Science Researcher ID: NA
- Scopus Author ID: NA
- Homepage: http://arakut.ac.ir/fa/asadi.html

How to cite this paper:
H. Salimi, A. Zakipour, M. Asadi, "A novel analytical approach for time-response shaping of the pi controller in field oriented control of the permanent magnet synchronous motors," J. Electr. Comput. Eng. Innovations, 10(2): 463-476, 2022.

DOI: 10.22061/JECEI.2022.8709.545

URL: https://jecei.sru.ac.ir/article_1694.html